Functional organization of 3D plant thylakoid membranes as seen by high resolution microscopy

Simona Streckaitė, Cristian Ilioaia, Igor Chaussavoine, Jevgenij Chmeliov, Andrius Gelzinis, Dmitrij Frolov, Leonas Valkunas, Sylvie Rimsky, Andrew Gall, Bruno Robert

BBA - Bioenergetics 1865 (2024) 149493

Contents lists available at ScienceDirect

BBA - Bioenergetics

journal homepage: www.elsevier.com/locate/bbabio

Functional organization of 3D plant thylakoid membranes as seen by high resolution microscopy

Simona Streckaite [a,b], Cristian Ilioaia [a], Igor Chaussavoine [a], Jevgenij Chmeliov [b,c], Andrius Gelzinis [b,c], Dmitrij Frolov [a], Leonas Valkunas [b,c], Sylvie Rimsky [d], Andrew Gall [a,*], Bruno Robert [a]

[a] Université Paris-Saclay, CEA, CNRS, Institute for Integrative Biology of the Cell (I2BC), 91198 Gif-sur-Yvette, France
[b] Department of Molecular Compound Physics, Center for Physical Sciences and Technology, Sauletekio av. 3, Vilnius 10257, Lithuania
[c] Institute of Chemical Physics, Faculty of Physics, Vilnius University, Sauletekio av. 9, Vilnius 10222, Lithuania
[d] CIRB – Collège de France, CNRS-UMR724, INSERM U1050, PSL Research University, 11 place Marcelin Berthelot, 75005 Paris, France

ARTICLE INFO

Keywords:
High-resolution fluorescence microscopy
Thylakoid membrane
Intact chloroplasts
3D thylakoid network
Stromal lamellae
Chlorophyll fluorescence

ABSTRACT

In the field of photosynthesis, only a limited number of approaches of super-resolution fluorescence microscopy can be used, as the functional architecture of the thylakoid membrane in chloroplasts is probed through the natural fluorescence of chlorophyll molecules. In this work, we have used a custom-built fluorescence microscopy method called Single Pixel Reconstruction Imaging (SPiRI) that yields a 1.4 gain in lateral and axial resolution relative to confocal fluorescence microscopy, to obtain 2D images and 3D-reconstucted volumes of isolated chloroplasts, obtained from pea (*Pisum sativum*), spinach (*Spinacia oleracea*) and *Arabidopsis thaliana*. In agreement with previous studies, SPiRI images exhibit larger thylakoid grana diameters when extracted from plants under low-light regimes. The three-dimensional thylakoid architecture, revealing the complete network of the thylakoid membrane in intact, non-chemically-fixed chloroplasts can be visualized from the volume reconstructions obtained at high resolution. From such reconstructions, the stromal connections between each granum can be determined and the fluorescence intensity in the stromal lamellae compared to those of neighboring grana.

1. Introduction

In plants, the process of photosynthesis originates in the internal membrane of the chloroplast organelle – the thylakoid membrane. It ensures the proper spatial organization of its constituent proteins. They include all the important players in the early steps of photosynthesis, responsible for light absorption and the subsequent energy transfer cascades as well as electron and proton transfer reactions: light-harvesting complexes, reaction centers, cytochrome b_6f, and ATP synthase (ATPase). Electron microscopy (EM) has been successfully used to reveal the internal organization of the thylakoid membrane. In the membrane of higher plants, it led to the discovery of the mainly photosystem II (PSII)-containing appressed regions, called grana, and the connecting regions that mainly contain photosystem I (PSI) and ATPase, called stromal lamellae [1]. The way these domains join together to form a continuous membrane system has been the subject of studies for several decades, and EM-based studies have led to a variety of 3D models. One of the most popular models is the helical model, according to which each granum is surrounded by multiple stroma lamellae, wrapping around the grana as right-handed helices [2]. Later EM serial sections and EM tomography studies seem to mostly confirm this helical model [3–5], which was recently further improved by 3D reconstructions [6]. It was shown that stroma thylakoids wind around grana as right-handed helices at an angle of about 16° relative to grana membranes, connecting to the grana thylakoids by staggered, fret-like protrusions. In addition, previously unreported left-handed helical surfaces were revealed at the interface between lamellar sheets [6]. While some stromal lamellae merge with the successive grana disks in short, 35-nm-wide, slit-like junctions, other junctions are up to 400-nm-wide, so that they form a planar sheet with only one grana disk [4]. Due to the tremendous technological progress, recent EM measurements no longer require the high level of preparation and fixation of the chloroplasts to

* Corresponding author.
E-mail address: Andrew.Gall@i2bc.paris-saclay.fr (A. Gall).

https://doi.org/10.1016/j.bbabio.2024.149493
Received 29 March 2024; Received in revised form 17 June 2024; Accepted 27 June 2024
Available online 5 July 2024

reveal their internal structural arrangement. Nonetheless, EM still does not yield crucial information on the functional organization of the photosynthetic systems under physiological, or near physiological conditions. This information, however, can be accessed at least partially, by 3D fluorescence imaging of the chlorophyll pigments, taking advantage of the fact that at room temperature most of the signal arises from PSII [7].

Such 3D fluorescence images of chloroplasts may help answering essential questions about the regulation of the energy flux during the first steps of photosynthesis. Even minor changes in the plant environment - light, water, temperature or nutrients – result in a fine-tuning of the set of reactions underlying the early steps of photosynthesis at timescales that range from seconds to months. These regulations adjust the amount of excitation energy collected by the light-harvesting proteins surrounding the reaction centers, ensure the balance of excitation energy between PSI and PSII, and also fine-tune the occurrence of cyclic electron transfer between PSI and cytochrome b_6f [8]. Short-term adaptations arise from local changes in light-harvesting proteins, which modify their ability to transfer excitation energy and eventually reorganize their spatial arrangement within the membrane [9], while long-term adaptations involve genetic regulations, which modify the overall protein composition of the thylakoid membrane [10]. The entire membrane organization of chloroplasts thus responds to environmental variations. For instance, the size and shape of the grana changes depend on the illumination conditions [11]. Several regulatory mechanisms are well documented at a molecular level [12], yet we still lack key knowledge of the response of the chloroplast membranes and especially of the role the latter play in these regulatory processes. An interplay must exist, however, between the different scales of the photosynthetic membrane organization, but it still remains to be clarified. For instance, the sensitivity of the granum structure to light environment has been established using EM [13–15]. In addition, a decade ago it was reported that the fast phase of the non-photochemical quenching process induces a subtle reorganization of the topology of the PSII proteins [16]. In general, unfortunately, our knowledge on these complex mechanisms remains scarce.

Ideally, live-cell imaging conditions should be used to visualize structures and processes *in vivo* or close to the native-state. Fluorescence imaging is a method of choice to analyze the photosynthetic membrane, without the need of specific staining or fluorescent-tagging procedures. Classical confocal microscopy has been used, yet the resolution of this method is limited by the Abbe limit to *ca.* 300 and 600 nm in lateral and axial directions, respectively. More recent super-resolution fluorescence imaging techniques overcome this diffraction limit and push the resolution to the nanoscale range. Successful attempts for thylakoid membrane imaging *in vivo* and *in situ* were provided using either super-resolution confocal live-imaging microscopy (SCLIM) [17] or methods derived from STED [18]. Recently, very detailed pictures of the photosynthetic membrane during some adaptation processes were obtained using three-dimensional structured illumination microscopy (3D-SIM) [19]. Although the resolution of such techniques is lower than that of EM, the information obtained *in vivo* and in real-time on chloroplast dynamics is highly complementary to the latter method. Indeed, it is essential for the holistic understanding of the thylakoid network function in ever-changing and challenging environments. SIM analysis of chloroplasts was particularly rich in new information. Nevertheless, none of these fluorescence-based techniques were able to yield precise 3D reconstructions of the thylakoid membrane.

In this work, we apply a novel fluorescence imaging method, termed single-pixel reconstruction imaging (SPiRI), to visualize the structure of the thylakoid membrane in plant chloroplasts. SPiRI is a variant of confocal microscopy, where the fluorescence is recorded by a detector smaller than the image of a point fluorophore. The use of such a small detector, provided its size is less than a third of the diffraction-limited image of a point-emitter, pushes confocal microscopy to its resolution limits, and yields a 1.4 gain in lateral and axial resolution, respectively, relative to classical confocal fluorescence microscopy depending on the excitation and emission wavelengths. In the presently applied conditions (*i.e.* exciting the sample with a 488 nm laser and recording the signal in the 660–700 nm range), its theoretical lateral and axial resolutions are 140 nm and 365 nm, respectively (see *Supplemental Material*), which leads to ~1.25 gain in lateral resolution. This approach easily yields 3D visualization of cellular structures, and in particular of the thylakoid structure in intact plant chloroplasts.

2. Methods

2.1. Plant growth

Spinach (*Spinacia oleracea*), pea (*Pisum sativum*) and Arabidopsis (*Arabidopsis thaliana*) plants were grown in growth cabinets (CLF Plant Climatics, Wertingen, Germany) under controlled light conditions, and in a greenhouse (I2BC Greenhouse Facility, Gif-sur-Vette, France). In growth cabinets under high-light (HL) conditions plants were submitted to 600 μmol photons $m^{-2}s^{-1}$ of white light illumination for 8 h per day. For low-light (LL) conditions the light intensity was reduced to 120 μmol photons $m^{-2}s^{-1}$ (8 h per day). Light in the growth cabinets was provided by Philips MASTER PL-L (Polar 55 W/840/4P 1CT) lamps.

2.2. Chloroplast preparation

Plant chloroplast isolation was performed at 4 °C temperature in the dark essentially as described previously [20]. In summary, sliced dark-adapted leaves (20–30 g) were homogenized in a blender for 5 s in 200 ml of a medium containing 300 mM sorbitol, 1 mM $MgCl_2$, 1 mM $MnCl_2$, 2 mM EDTA, 30 mM KCl, 0.5 mM KH_2PO_4 and 50 mM MES-KOH (pH = 6.1). The obtained mixture was filtered through six layers of cheesecloth and centrifuged at 2000*g* for 2 min. The pellet obtained after centrifugation was resuspended in the same medium and centrifuged again at 2000*g* for 2 min. The new pellet was resuspended in the same medium poised at pH = 7.6, and centrifuged at 2500*g* for 3 min. The final pellet, containing intact chloroplasts, was then resuspended in 1–2 ml of the same medium.

2.3. Microscopy

Microscopy was performed at room temperature on a custom-built set-up, equivalent to a confocal microscope, but providing ~1.4 higher resolution in all three dimensions (see *Supplemental Material*). Samples (5 μl) were sandwiched in between two round cover slips of 22 mm diameter, the bottom one being coated with Corning® Cell-Tak™ to provide chloroplast attachment to the glass. The coverslip sandwiches were then sealed with nail varnish to prevent drying and housed in a custom-made sample holder. The sample holder was fixed to a nano-positioning system (P-733.2CD, P-725.4CD, E-725.3CD; Physik Instrumente) coupled to an inverted Ti-U microscope (Nikon). As in laser-scanning confocal microscopy, samples were scanned by a 488 nm LX OBIS (Coherent) focused laser beam (100 nW at the sample) that was collimated prior to focusing with a spatial filter assembly (KT310, LA1986-A; Thorlabs). The 660–700 nm fluorescence emission signal was recorded in backscattering geometry using a dichroic mirror (59022BS, Chroma Technology)/emission filter doublet (FF01-679/41-25, Semrock), essentially monitoring PSII emission. Nikon CFI PLAN APO objective lenses (60× air, 100× oil) were used both to focus the beam and to collect the emitted signal. The fluorescence emission signal was recorded with an iXon Ultra 978 EMCCD camera (Andor) coupled to a custom-made Optomask (Cairn Research Ltd). The dwell time at each recorded pixel position was 30 ms.

2.4. Image treatment

Recorded images were constructed from the fluorescence intensity

recorded at the central pixel of CCD camera. Deconvolution was carried out with a plug-in implemented in Fiji by using the Richardson-Lucy algorithm with total-variation regularization [21,22]. Each 2D plane was deconvolved by using the regularization parameter set to 10^6 and 10 iterations were performed during the algorithm's run with experimentally obtained PSF of (full-width-at-half-maximum) $FWHM_{x:y} = 180$: 180 nm. Volumetric 3D reconstruction from deconvolved 2D planes was performed with Volume Viewer (Kai Uwe Barthel, Internationale Medieninformatik) plug-in implemented in Fiji. Background from all the images was removed by using custom-written R [23] scripts.

2.5. Grana diameter evaluation

Firstly, one granum was selected from the SPiRI image of the whole chloroplast and fitted by a two-dimensional (2D) Gaussian function: $z = z_0 + A \exp.[-0.5((x\text{-}x_c)/w_1)\ [2]\text{–}0.5((y\text{-}y_c)/w_2)\ [2]]$. Secondly, the grana diameter was determined as FWHM of the 2D Gaussian fit of the obtained granum image (see Fig. S2). All the grana diameters were evaluated from the intact chloroplasts isolated from plants grown under the same conditions for HL and LL cases. Only upper young leaves of the plants were used for chloroplast isolation, and imaging conditions were identical: 100× oil objective, 488 nm laser excitation, 660–700 nm emission range, 50 nm x&y scanning step sizes. Around 50 grana stacks were evaluated from several chloroplasts for each of the plant growth conditions.

3. Results and discussion

3.1. SPiRI 2D-imaging of chloroplasts

The representative fluorescence images of intact chloroplasts that were extracted from pea (*Pisum sativum*), spinach (*Spinacia oleracea*), and *Arabidopsis thaliana*, grown under low-light conditions (see *Methods*), and visualized using our SPiRI microscope, are shown in Fig. 1. In these images, very clear grana stacks—the bright round structures—can be observed due to the high slicing power of our approach, in contrast to super-resolution confocal live imaging microscopy (SCLIM), which shows poor visualization of the grana and stromal structures [17]. Altogether, these images are quite similar to recent pictures obtained by SIM for spinach [24] and *Arabidopsis* [19] chloroplasts; the size and shape of the fluorescent spots corresponding to the grana stacks differ slightly between species. In agreement with previous studies, pea chloroplasts exhibit less clear grana and stromal structures when compared to spinach and *Arabidopsis* chloroplasts [24,25].

A series of intact chloroplasts were prepared from plants (spinach and *Arabidopsis*) grown under different light conditions. Defined low-light (LL) and high-light (HL) environments were provided by growth cabinets, and natural fluctuating light by the green house. For each chloroplast, the microscope focus was adjusted on to a single plane, where the most intense signal arises from the grana. This plane is usually close to the center of the chloroplast, where several grana display clear margins. Each grana section observed in this plane was fitted with a 2D Gaussian function (see *Methods*), and the grana diameter was calculated as an average of the FWHM of this Gaussian along the x and y dimensions. This process allows a numerical determination of the grana diameter distribution depending on the growth conditions or the plant species considered, that is shown in Fig. 2.

The calculated diameters of grana show a spread for all light conditions used. The average diameter of grana in chloroplasts from spinach grown under LL is 420 nm, and this value decreases for HL grown spinach to 370 nm. In chloroplasts extracted from spinach grown under fluctuating light conditions (greenhouse), the grana diameter was similar to that observed using HL conditions. Using confocal laser scanning microscopy (CLSM), the grana diameter in chloroplasts of *Arabidopsis* grown under similar LL conditions (100 μmol photons $m^{-2}s^{-1}$, 9 h per day), was first determined to be 370 nm[13], but this value was later corrected by EM and biochemical data to around 440 nm[14], *i.e.* the same value which we determine directly using SPiRI microscopy. In chloroplasts extracted from spinach grown using an illumination of 200 μmol photons $m^{-2}s^{-1}$ for 12 h per day, the average grana diameter of 390 nm was reported using SIM [24]. From our experiments, we estimate that fivefold increase of the light intensity used for plant growth (120 μmol photons $m^{-2}s^{-1}$ for LL *vs.* 600 μmol photons $m^{-2}s^{-1}$ for HL conditions) results in a grana diameter decrease from 420 nm to 370 nm

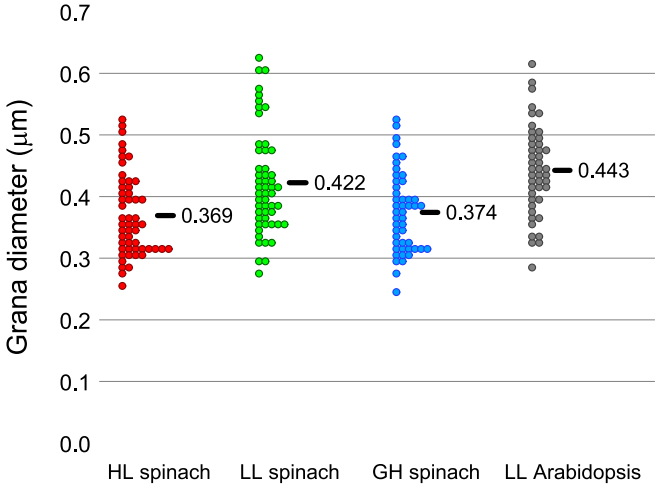

Fig. 2. Spinach and Arabidopsis grana diameter dependence on the plant growth conditions. The numerical value next to the data points is the average grana diameter for each of the conditions. LL – low-light, HL – high-light, GH - greenhouse.

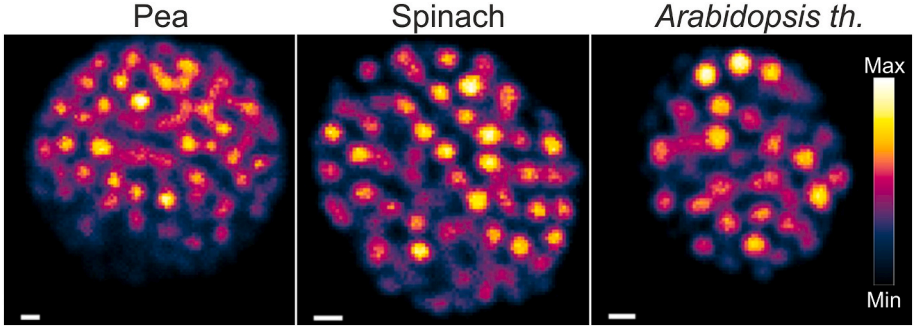

Fig. 1. Thylakoid organization in chloroplasts of pea, spinach and Arabidopsis from low-light-grown plants. Pea chloroplasts were scanned with 80 nm x&y steps, using a 60× objective. Spinach and Arabidopsis chloroplasts were scanned with 60 nm x&y steps, using a 100× objective; all the samples were excited at 488 nm. Scale bar in all images is 500 nm.

– of about 14 % (see Fig. 2). The values obtained using SIM [24] match our measurements of grana diameter quite well, as for around 1.7 times higher light intensity (200 μmol photons $m^{-2}s^{-1}$ for SIM experiments *vs.* 120 μmol photons $m^{-2}s^{-1}$ for our experiments) we expect 5 % smaller diameters of around 400 nm. Considering that our LL illumination lasted for a 4 h-shorter period of time, which could induce a bit larger granum, the values of our grana diameters are in a good agreement with the ones reported previously.

3.2. 3D reconstruction of the Arabidopsis thylakoid membrane

The microscopy method used in this work can be described as classical confocal microscopy, where the signal is measured using an infinitely small pinhole (see *Supplemental Material*). Accordingly, it possesses the flexibility of confocal microscopy, and, in particular, allows easy volumetric reconstruction of the chloroplast, which is obtained from fluorescence recorded on successive planes. Fig. 3A illustrates the fluorescence signal obtained at different planes separated by 300 nm (a distance corresponding to about the axial resolution of the method) of an intact chloroplast extracted from LL-grown *Arabidopsis*. This ensemble of 2D planes, extending over nearly two micrometers, spans most of the chloroplast. The corresponding reconstructed volumetric image of the chloroplast is shown if Fig. 3B.

The obtained volumetric reconstruction of the thylakoid network can be analyzed from any direction.

Fig. 3C illustrates a lateral view of the chloroplast, which can be generated from the reconstructed volume. Slicing the 3D chloroplast image from the side, grana appear as elongated cylinders (around 700–800 nm in length and around 370–510 nm in width), preferentially oriented parallel to the optical axis of the microscope. The stacked areas, however, are irregular, sometimes merging with each other and not always being parallel one to another as typically depicted, or modelled, from the EM data [4]. Up to now, the only models available for the 3D visualization of thylakoid architecture in native chloroplasts have been obtained by CLSM for plants [25,26] and by SCLIM for moss [17]. In these 3D visualizations we cannot distinguish clear grana and stroma domains for pea, bean [25,26] and *Physcomitrella patens* [17], although they were observable in 2D images. This is likely due to the limited axial resolution of the confocal microscopy methods used to produce the volumes of the thylakoid network.

Using SPiRI, the stromal connections between each granum can be determined. For example, in Fig. 3C, the stromal connection between two successive grana (yellow dotted lines) are underlined by a pink dotted line. By following these lines in consecutive images, the ensemble of the continuous network between grana and stromal lamellae is observed. We estimate that a bit more than half of the stromal lamellae are connected to the grana at an angle of about 155 ± 11° and the rest at an angle of about 135 ± 5° (see also Fig. 4). This result is consistent with

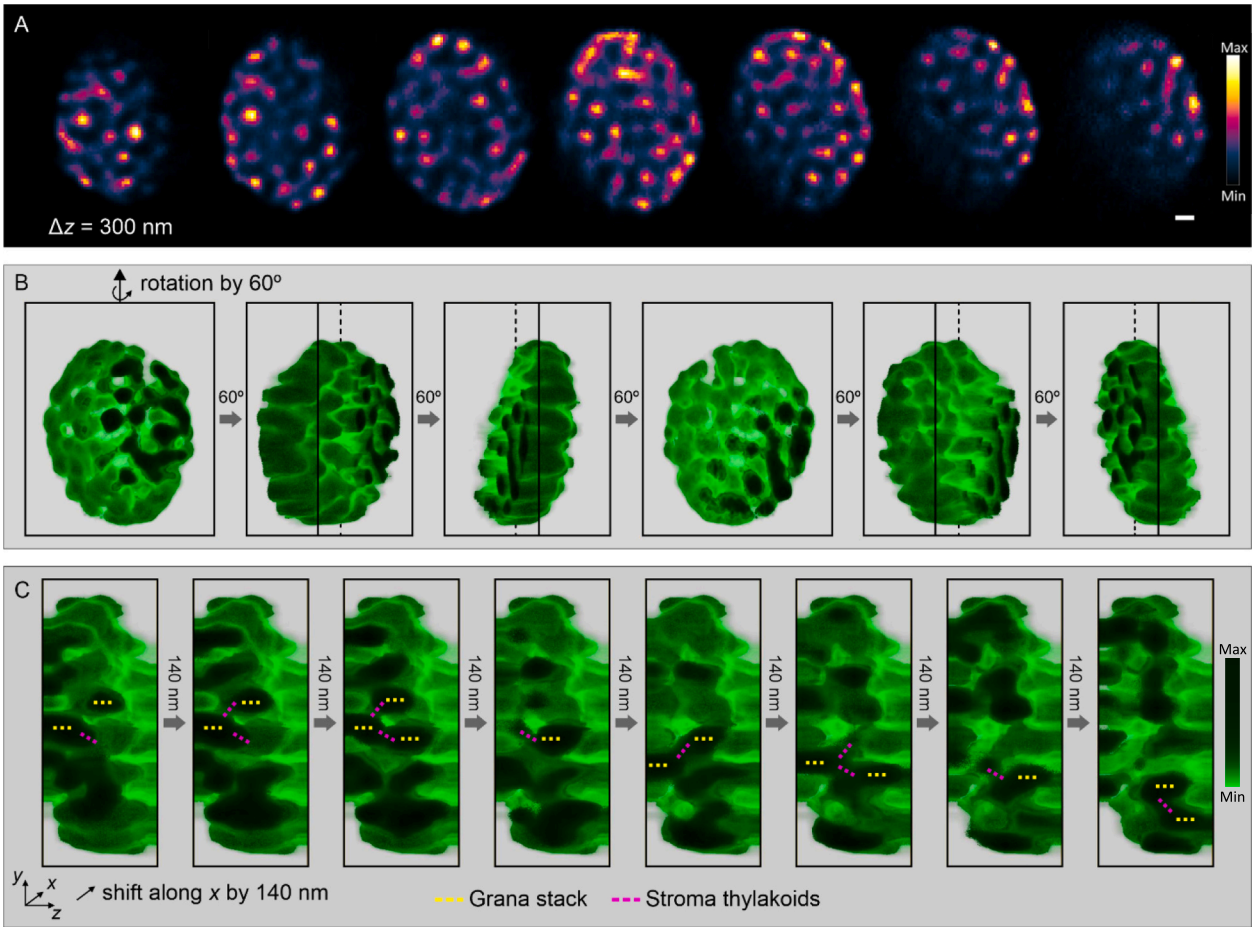

Fig. 3. A: Fluorescence signal obtained at different planes separated by 300 nm from an intact chloroplast extracted from Arabidopsis grown under low-light conditions. Horizontal scale bar at the bottom right corner is 500 nm. B: Views of the reconstructed volume (from the recorded 7 planes in A) obtained by the successive rotation of 60°. C: Cross-sections of the reconstructed volume from the side view sliced every 140 nm in the x direction. In C, the continuous network of grana and stroma lamellae can be observed by following the yellow (grana) and pink (stroma lamellae) lines in the sequential images. In B and C, the fluorescence intensity is color-coded varying from light green (low fluorescence intensity) to dark green (high fluorescence intensity). The chloroplast was scanned with 70 nm x&y, and 300 nm z steps with an 100× objective. The sample was excited at 488 nm and emission collected in the 660–700 nm range. (For interpretation of the references to color in this figure legend, the reader is referred to the web version of this article.)

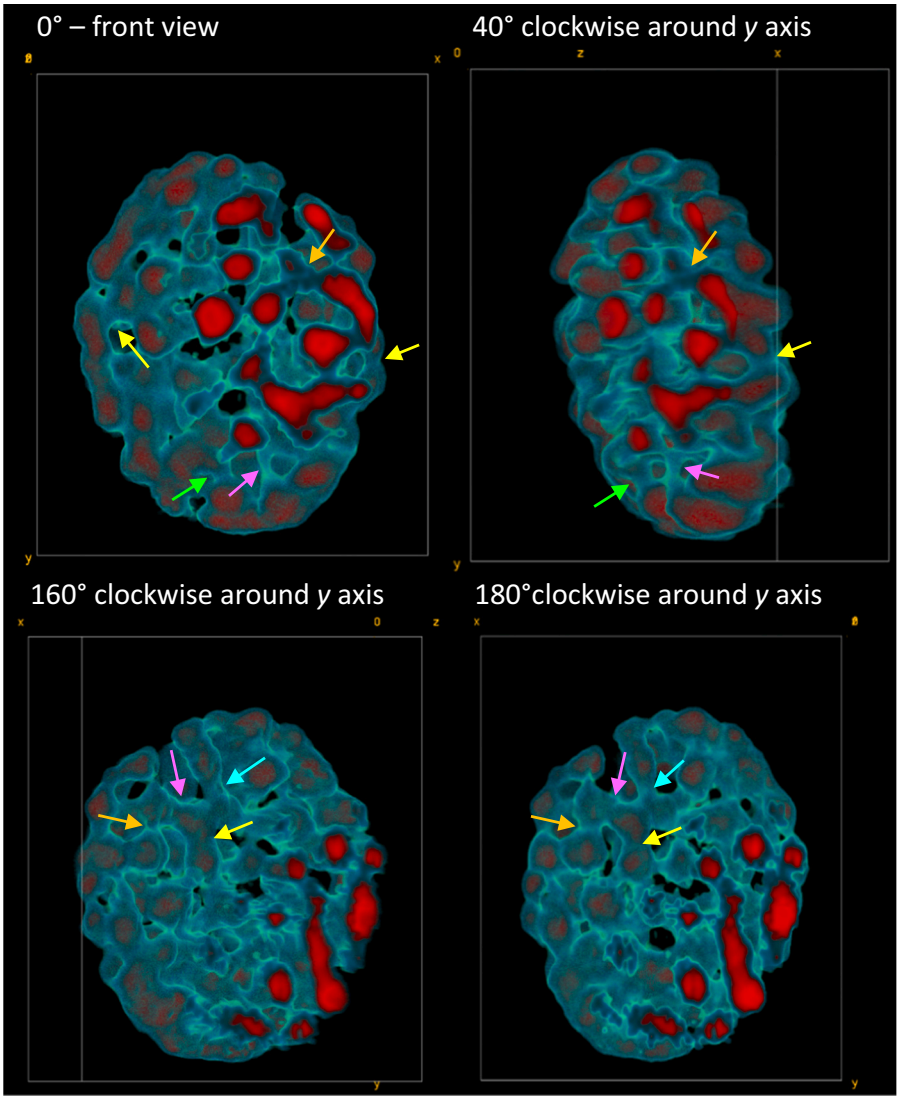

Fig. 4. The 3D reconstruction (false colors) of the thylakoid network in an Arabidopsis chloroplast. The red color represents the most intense fluorescence signal, and teal low intensities. The colored arrows correspond to the same spot of the grana connections in adjacent images. The chloroplast was scanned with 70 nm x&y, and 300 nm z steps with an 100× objective in the 660–700 nm emission range. The sample was excited at 488 nm. (For interpretation of the references to color in this figure legend, the reader is referred to the web version of this article.)

the helical structure model, however, from volumetric reconstruction of these fluorescence images, it is hard to say if stroma lamellae wind around the grana. On the other hand, we can clearly observe stroma lamellae as extensions connecting one granum with another.

The 3D reconstructions can also follow the fluorescence intensity in the stromal lamellae. As this can be clearly observed in the volumetric reconstruction, the fluorescence intensity associated to these regions can be determined. As absolute fluorescence measurements may depend on the depth of the fluorescing site location in the chloroplast, we chose to compare the stromal fluorescence intensity to that of the proximal grana. We found that the fluorescence intensity of stroma lamellae is always significantly lower than the intensity of the proximal grana. This can be observed in Fig. 4, where the chloroplast volume is built with the contrasting colors for high and low fluorescence intensity to better visualize the three-dimensional thylakoid architecture, revealing the network of the thylakoid membrane in intact, non-chemically-fixed chloroplasts. In this 3D thylakoid network, stromal connections are shown by arrows, the most intense emission being represented in red and least intense by teal. We estimate that the fluorescence intensity in stroma lamellae is between 60 and 75 % lower than that of their connected grana. This can be visualized using different fluorescence intensity thresholds, as shown in Fig. 5. The fluorescence intensity in SpiRI images of successive planes from an *Arabidopsis* chloroplast are presented by three thresholds, where the 0–25 % of the lowest values of the signal (white) represents background and corresponds to the rest of the chloroplast volume, which is not assigned to the grana or stroma lamellae in the particular imaged plane. The 25–43 % range of the signal (teal) represents well the connections between grana, which are shown as 43–100 % of the highest signal values (red). Such visualizations of the intensity distribution is in a good agreement with the fluorescence images, where we observe the connecting stromal lamellae between the neighboring grana.

These experiments confirmed that the fluorescence intensity of stromal lamellae is quite heterogeneous, as it was possible to reconstruct the whole network only when a threshold ranging from 25 to 43 % of the grana intensity was used. Considering that our detection filter has a 660–700 nm range, where the detected fluorescence arises from photosystem II, this indicates the presence of sizeable (although variable) amounts of these proteins in the stromal lamellae. Furthermore, the fluorescence of each stromal lamellae seems constant along the

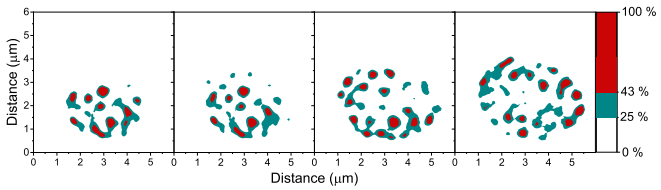

Fig. 5. Fluorescence intensity recorded from successive planes (every 300 nm) of an Arabidopsis chloroplast. False color images show where thylakoid membrane domains with a threshold of 25–43 % of the grana intensity are used to visualize the stromal lamellae. Grana are shown in red and stroma lamellae in teal. The chloroplast was scanned with 70 nm x&y, and 300 nm z steps with an 100× objective in the 660–700 nm emission range while exciting at 488 nm. (For interpretation of the references to color in this figure legend, the reader is referred to the web version of this article.)

lamellae axis, suggesting a probable homogeneity of the concentration of these proteins within the stroma lamellae.

4. Conclusions

In this present work, we have shown that the relatively simple laser-scanning microscopy method, SPiRI, is able to obtain a better resolution than the theoretical resolution of confocal fluorescence microscopy. Due to the resolution gain, and to the possibility of easy volumetric reconstruction from sequential plane scanning, it yields original information on the structure of the thylakoid membrane in intact, non- chemically-fixed, chloroplasts. It thus represents a promising technique to explore at the mesoscopic scale the overall volumes of grana/stroma lamellae and their evolution during plant adaptation to their environment.

CRediT authorship contribution statement

Simona Streckaite: Writing – review & editing, Writing – original draft, Visualization, Validation, Investigation, Formal analysis, Data curation. **Cristian Ilioaia:** Writing – review & editing, Supervision, Methodology, Investigation, Formal analysis, Data curation, Conceptualization. **Igor Chaussavoine:** Visualization, Software. **Jevgenij Chmeliov:** Writing – review & editing, Visualization, Validation, Software, Formal analysis. **Andrius Gelzinis:** Writing – review & editing, Software, Formal analysis. **Dmitrij Frolov:** Software, Methodology. **Leonas Valkunas:** Writing – review & editing, Methodology, Formal analysis. **Sylvie Rimsky:** Methodology, Conceptualization. **Andrew Gall:** Writing – review & editing, Validation, Supervision, Software, Methodology, Formal analysis, Data curation, Conceptualization. **Bruno Robert:** Writing – review & editing, Writing – original draft, Validation, Supervision, Methodology, Funding acquisition, Formal analysis, Data curation, Conceptualization.

Declaration of competing interest

Cristian Ilioaia, Dmitrij Frolov, Andrew Gall, Bruno Robert reports financial support was provided by I2BC through the French Infrastructure for Integrated Structural Biology. Cristian Ilioaia, Andrew Gall, Bruno Robert reports financial support was provided by Infrastructures en Biologie Santé et Agronomie. Simona Streckaite, Jevgenij Chmeliov, Andrius Gelzinis, Leonas Valkunas reports financial support was provided by Research Council of Lithuania. Cristian Ilioaia, Dmitrij Frolov, Andrew Gall, Igor Chaussavoine, Bruno Robert reports a relationship with Eloquant Nanoimaging that includes: board membership, employment, and equity or stocks. Bruno Robert, Andrew Gall, Dmitrij FROLOV has patent #Imaging method, and system, for obtaining a super-resolution image of an object (US10527837B2) issued to Centre National de la Recherche Scientifique CNRS Commissariat a lEnergie Atomique et aux Energies Alternatives CEA. If there are other authors, they declare that they have no known competing financial interests or personal relationships that could have appeared to influence the work reported in this paper.

Data availability

Data will be made available on request.

Acknowledgements

We thank Anja Krieger-Liszkay (Institute of Integrative Biology of the Cell (I2BC), CEA/CNRS/Université Paris-Saclay, Gif-sur-Yvette cedex, France) for her aid in chloroplast isolation and the greenhouse facility at the I2BC. This work was supported by the platform of Biophysics of the I2BC through the French Infrastructure for Integrated Structural Biology (FRISBI; grant number ANR-10-INSB-05), the Infrastructures en Biologie Santé et Agronomie (IBiSA) and the Research Council of Lithuania (LMT Grant No. S-MIP-23-31).

Appendix A. Supplementary data

Supplementary data to this article can be found online at https://doi.org/10.1016/j.bbabio.2024.149493.

References

[1] D.J. Paolillo, The three-dimensional arrangement of intergranal lamellae in chloroplasts, J. Cell Sci. 6 (1970) 243–255.
[2] L. Mustárdy, G. Granum Garab, revisited., A three-dimensional model - where things fall into place, Trends Plant Sci. 8 (2003) 117–122.
[3] L. Mustárdy, K. Buttle, G. Steinbach, G. Garab, The three-dimensional network of the thylakoid membranes in plants: quasihelical model of the granum-stroma assembly, Plant Cell 20 (2008) 2552–2557.
[4] J.R. Austin, L. Andrew Staehelin, Three-dimensional architecture of grana and stroma thylakoids of higher plants as determined by electron tomography, Plant Physiol. 155 (2011) 1601–1611.
[5] E. Shimoni, O. Rav-Hon, I. Ohad, V. Brumfeld, Z. Reich, Three-dimensional organization of higher-plant chloroplast thylakoid membranes revealed by electron tomography, Plant Cell 17 (2005) 2580–2586.
[6] Y. Bussi, et al., Fundamental helical geometry consolidates the plant photosynthetic membrane, Proc. Natl. Acad. Sci. U. S. A. 116 (2019) 22366–22375.
[7] Govindje., Sixty-three years since Kautsky: chlorophyll a fluorescence, Funct. Plant Biol. 22 (1995) 131–160.
[8] R.E. Blankenship, Molecular Mechanisms of Photosynthesis, 2nd edition, JohnWiley & Sons, Ltd, 2014.
[9] A. Ruban, The Photosynthetic Membrane: Molecular Mechanisms and Biophysics of Light Harvesting vol. 267, John Wiley & Sons, Ltd., 2013.
[10] J. Anderson, W. Chow, D. Goodchild, Thylakoid membrane organisation in sun/shade acclimation, Aust. J. Plant Physiol. 15 (1988) 11–26.
[11] M. Pribil, M. Labs, D. Leister, Structure and dynamics of thylakoids in land plants, J. Exp. Bot. 65 (2014) 1955–1972.
[12] R. Arshad, et al., A kaleidoscope of photosynthetic antenna proteins and their emerging roles, Plant Physiol. 189 (2022) 1204–1219.
[13] M. Herbstová, S. Tietz, C. Kinzel, M.V. Turkina, H. Kirchhoff, Architectural switch in plant photosynthetic membranes induced by light stress, Proc. Natl. Acad. Sci. U. S. A. 109 (2012) 20130–20135.
[14] S. Puthiyaveetila, et al., Compartmentalization of the protein repair machinery in photosynthetic membranes, Proc. Natl. Acad. Sci. U. S. A. 111 (2014) 15839–15844.
[15] T. Schumann, S. Paul, M. Melzer, P. Dörmann, P. Jahns, Plant growth under natural light conditions provides highly flexible short-term acclimation properties toward high light stress, Front. Plant Sci. 8 (2017) 1–18.
[16] M.P. Johnson, A.P.R. Brain, A.V. Ruban, Changes in thylakoid membrane thickness associated with the reorganization of photosystem II light harvesting complexes during photoprotective energy dissipation, Plant Signal. Behav. 6 (2011) 1386–1390.
[17] M. Iwai, M. Yokono, K. Kurokawa, A. Ichihara, A. Nakano, Live-cell visualization of excitation energy dynamics in chloroplast thylakoid structures, Sci. Rep. 6 (2016) 1–10.
[18] J. Bierwagen, et al., Far-field autofluorescence nanoscopy, Nano Lett. 10 (2010) 4249–4252.
[19] M. Iwai, M.S. Roth, K.K. Niyogi, Subdiffraction-resolution live-cell imaging for visualizing thylakoid membranes, Plant J. 96 (2018) 233–243.
[20] M. Messant, et al., Glycolate induces redox tuning of photosystem II in vivo: study of a photorespiration mutant, Plant Physiol. 177 (2018) 1277–1285.
[21] W.H. Richardson, Bayesian-based iterative method of image restoration*, J. Opt. Soc. Am. 62 (1972) 55–59.
[22] L.B. Lucy, An iterative technique for the rectification of observed distributions, Astron. J. 79 (1974) 745–754.

[23] R Core Team, A Language and Environment for Statistical Computing, R Foundation for Statistical Computing, Vienna, Austria, 2020 (www.R-project.org/).
[24] W.H.J. Wood, S.F.H. Barnett, S. Flannery, C.N. Hunter, M.P. Johnson, Dynamic thylakoid stacking is regulated by LHCII phosphorylation but not its interaction with PSI, Plant Physiol. 180 (2019) 2152–2166.
[25] I. Rumak, et al., Correlation between spatial (3D) structure of pea and bean thylakoid membranes and arrangement of chlorophyll-protein complexes, BMC Plant Biol. 12 (2012) 1–18.
[26] I. Rumak, et al., 3-D modelling of chloroplast structure under (Mg2+) magnesium ion treatment. Relationship between thylakoid membrane arrangement and stacking, Biochim. Biophys. Acta Bioenerg. 1797 (2010) 1736–1748.